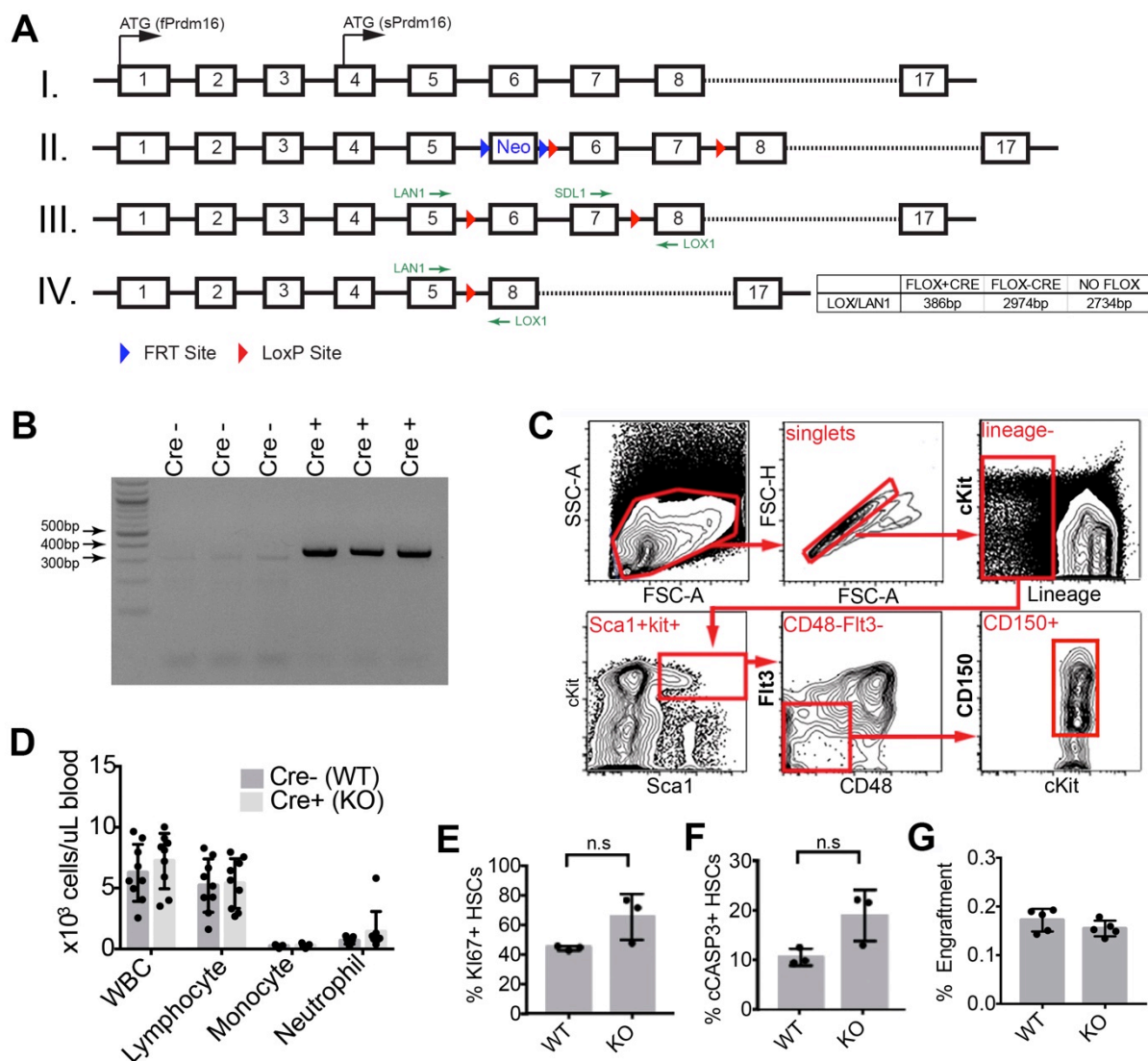
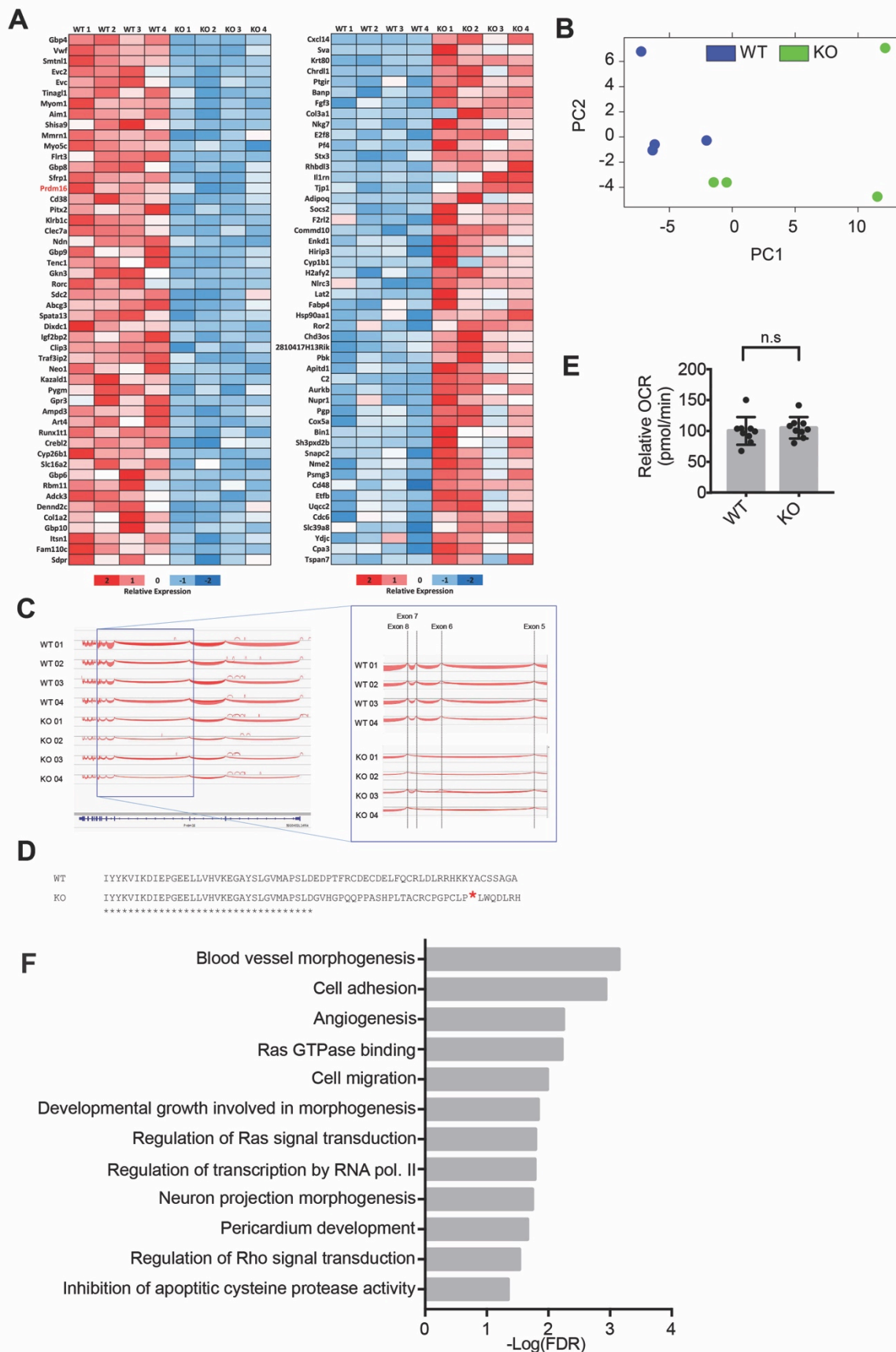




**Figure S1: Genomic structure and conservation of PRDM16.** Alignment of primary amino acid sequences of short and full PRDM16 isoforms from human and mouse. Alignment performed using ClustalW2 multiple sequence alignment. Asterisks (\*) indicate fully-conserved residues, colons (:) indicate strong conservation with scoring of  $>0.5$  using the PAM250 matrix. Periods (.) represent weak conservation with scoring of  $\leq 0.5$ . Conserved domains are colored as follows – SET methyltransferase (PR) domain (yellow), Zn-finger DNA binding domains (green, two hues to indicate distinct adjacent domains), proline-rich domain (red), CtBP binding domain motifs (fully-conserved PFDLT and PLDLS sequences) (violet), acidic domain (blue). Of note is the absence of nearly all of the PR domain in the short mouse and human isoforms and the strong conservation overall between human and mouse.

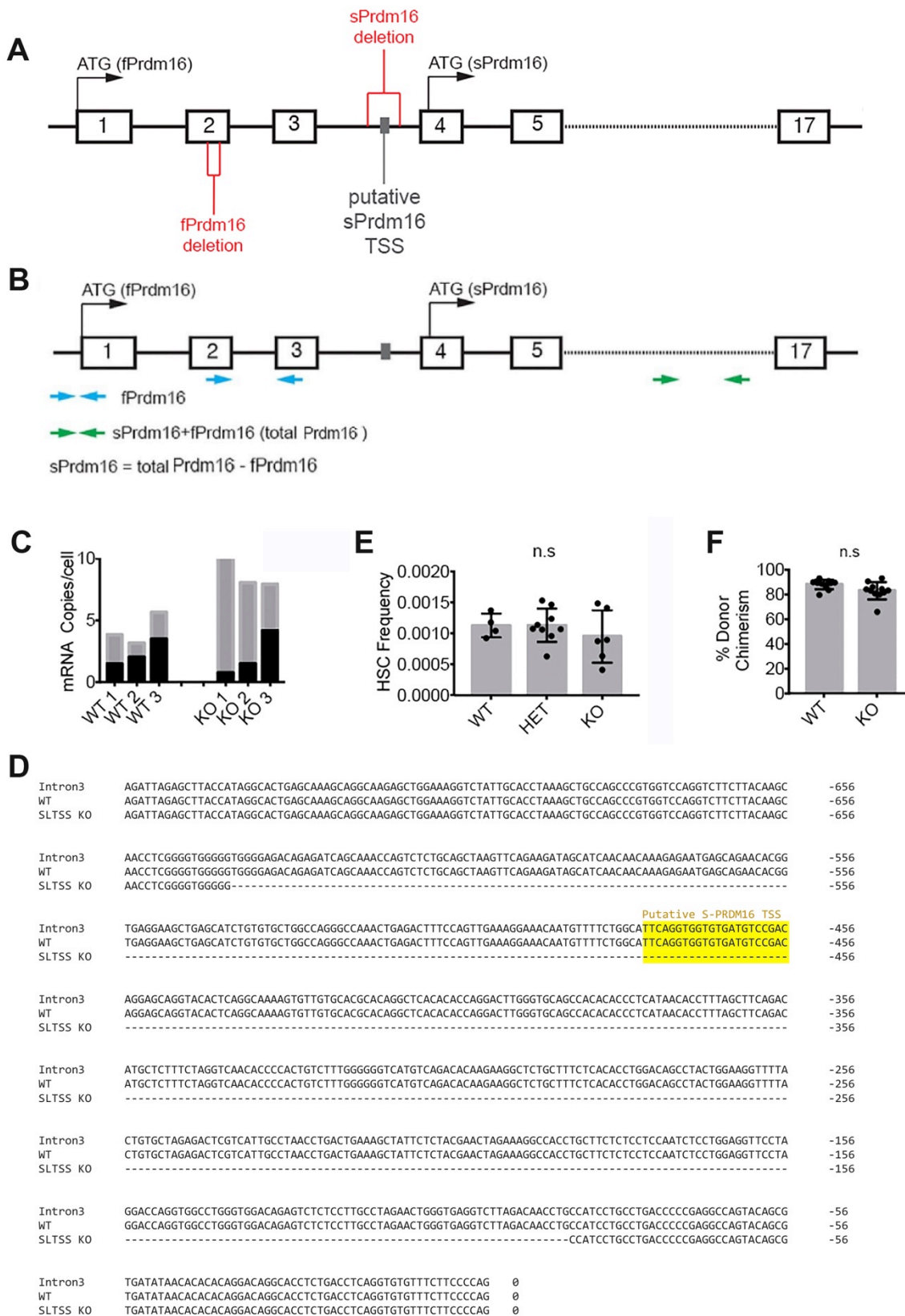


**Figure S2: Generation and phenotype of *Prdm16<sup>fl/fl</sup>.Vav-Cre* mice. (A)** Schematic representation of the generation of *Prdm16<sup>fl/fl</sup>* mice – I. Map of *Prdm16* exons and introns, including the two start codons for *fPrdm16* and *sPrdm16*, respectively. II. Insertion of a Neomycin-resistance cassette flanked by FRT sites, and of LoxP sites around exons 6 and 7. III. Map of the *Prdm16<sup>fl/fl</sup>* genomic structure after removal of the Neo cassette by crossing to a FLP-recombinase<sup>+/-</sup> mouse, with the highlighting (in green) of LAN1, SDL1, and LOX1 primers for use in genotyping. IV. Deletion of *Prdm16* exon 6 and 7 in the presence of Cre recombinase, with LAN1/LOX1 locations and a table illustrating differences in LOX1/LAN1 amplicon length with or without genomic excision. **(B)** LOX1/LAN1 PCR of hematopoietic PB cells from three Cre<sup>-</sup> and three Cre<sup>+</sup> mice showing the presence of a 380bp amplicon in the excised mice. **(C)** Gating scheme of adult BM HSCs (Lin<sup>-</sup>cKit<sup>+</sup>Sca<sup>+</sup>Flt3<sup>-</sup>CD48<sup>-</sup>CD150<sup>+</sup>) **(D)** Blood counts for white blood cells (WBC), lymphocytes, monocytes and neutrophils in peripheral blood of *Vav-Cre<sup>-/-</sup>Prdm16<sup>fl/fl</sup>* (WT) and *Vav-Cre<sup>+/-</sup>Prdm16<sup>fl/fl</sup>* (KO) mice. ( $n = 9$ ). **(E)** Percentage of Ki67<sup>+</sup> and **(F)** Cleaved caspase3<sup>+</sup> BM HSCs from WT and KO mice ( $n = 3$ ). **(G)** Percent of WT or KO donor CD45.2 cells in BM of recipient mice 24-hours post-transplant. ( $n = 5$  recipient mice). (n.s. =  $P > 0.05$ ).

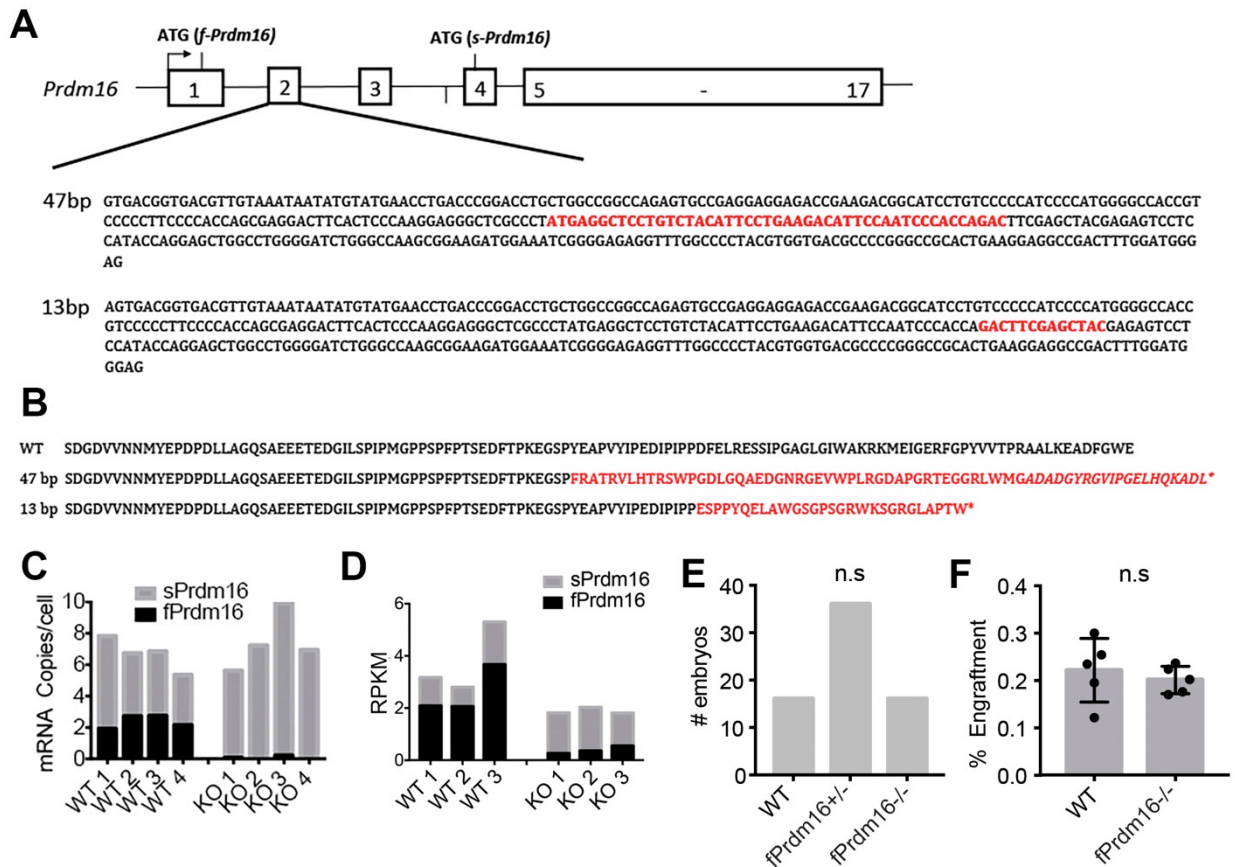


**Figure S3: Genome-wide expression analysis of *Prdm16<sup>fl/fl</sup>.Vav-Cre* mice** (A) Heatmap of the top 50 genes (by *P*-value) up/downregulated in *Vav-Cre<sup>+/-</sup> Prdm16<sup>fl/fl</sup>* (KO) BM HSCs and WT littermate BM HSC samples, as determined by RNAseq. (B) Principal component analysis (PCA) of individual WT and KO RNAseq samples (C) Quantification of *Prdm16* exons in RNAseq analysis of *Prdm16<sup>fl/fl</sup>.Vav-Cre* and WT littermate HSCs using the Integrative Genomics Viewer (IGV) showing absence of reads at exons 6 and 7 in KO samples. (D) Analysis of *Prdm16<sup>fl/fl</sup>.Vav-Cre* and WT littermate PRDM16 amino acid sequences showing a frameshift and early termination 25 amino acids downstream of the C-terminus of exon 5. (E) Basal oxygen consumption rate (OCR) of WT and KO mouse embryonic fibroblasts (MEFs) ( $n = 3$  experiments with technical triplicates) (n.s. =  $P > 0.05$ ) (F) GO pathways significantly downregulated in sorted  $\text{Lin}^{-}\text{cKit}^{+}\text{Sca}^{+}\text{Flt3}^{-}\text{CD48}^{-}$  *Prdm16<sup>fl/fl</sup>.Vav-Cre* FL HSCs compared to WT littermates. Values expressed as  $-\text{Log}_{10}$  of the *P*-value, determined by PANTHER RNAseq analysis.



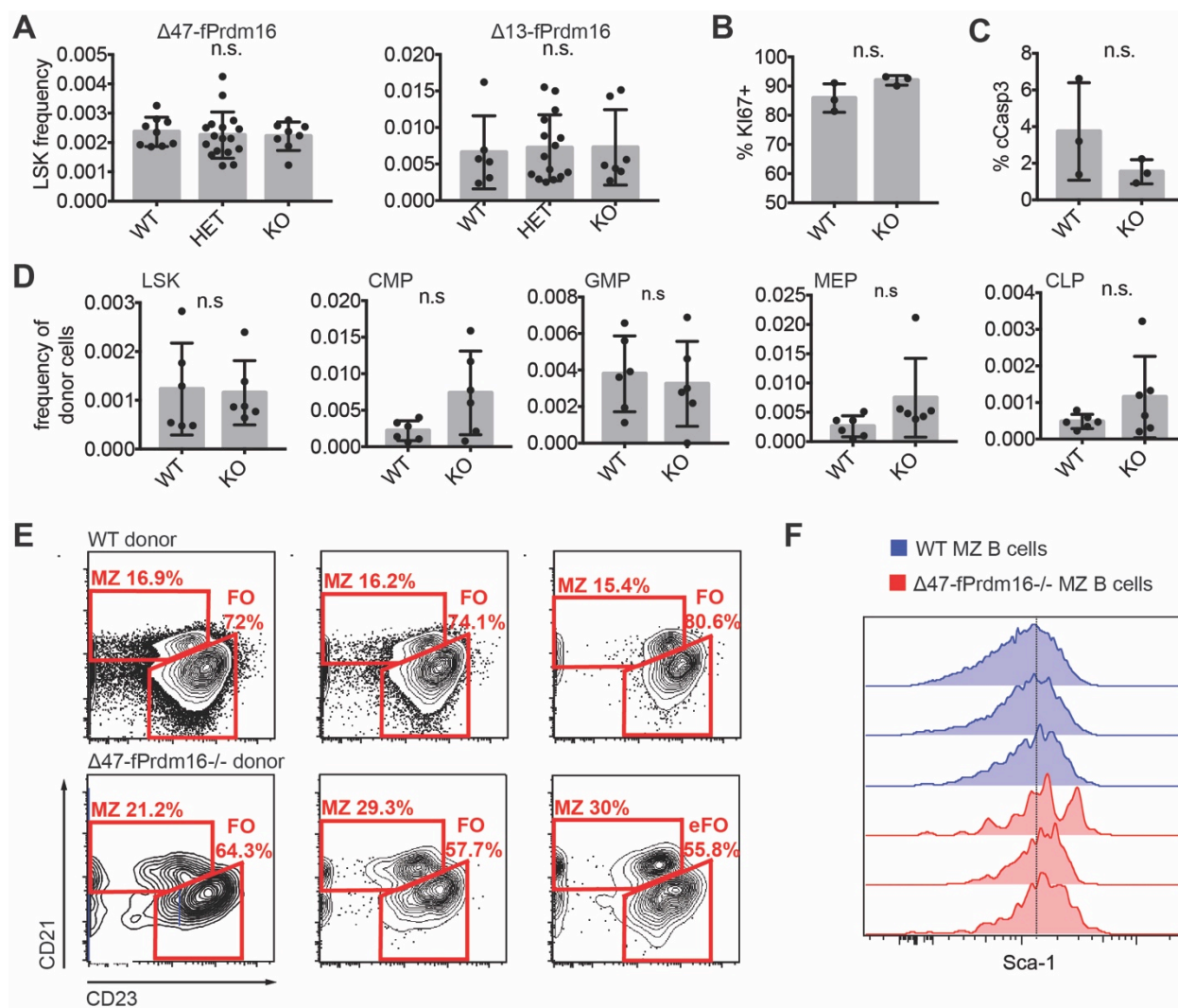


**Figure S4: Targeting of *sPrdm16* TSS.** (A) Schematic representation of regions targeted in CRISPR/Cas9 *Prdm16* isoform-deletion experiment, highlighting exon structure, *fPrdm16* and *sPrdm16* start codons, and putative *sPrdm16* TSS in intron 3. (B) Schematic of subtractive qPCR used to determine copy number of *sPrdm16* mRNA. Probes in exon 2/3 are specific for *fPrdm16* and probes in exon14/15 are used to calculate total *Prdm16*. *sPrdm16* is calculated by subtracting *fPrdm16* from *tPrdm16*. (C) Quantification based on subtractive qPCR of *Prdm16* isoform copy number from mice deleted for the *sPrdm16* putative TSS (KO) compared to WT littermates. (D) FL HSC frequency in WT, KO, or TSS-heterozygous (HET) mice. (E) Peripheral blood (PB) donor chimerism of transplanted WT or KO BM HSCs in competitive transplants with CD45.1 BM, measured 16-weeks post-transplant ( $n = 10-11$  recipients from 3 independent experiments). (F) Alignment of sequencing results from intron 3 of a WT mouse and a putative *sPrdm16*-TSS KO (SLTSS KO). Sequencing results are aligned to the final 755 nucleotides of *Prdm16* intron 3 and illustrate loss of the putative *sPrdm16* TSS from the SLTSS KO mice, highlighted in yellow.

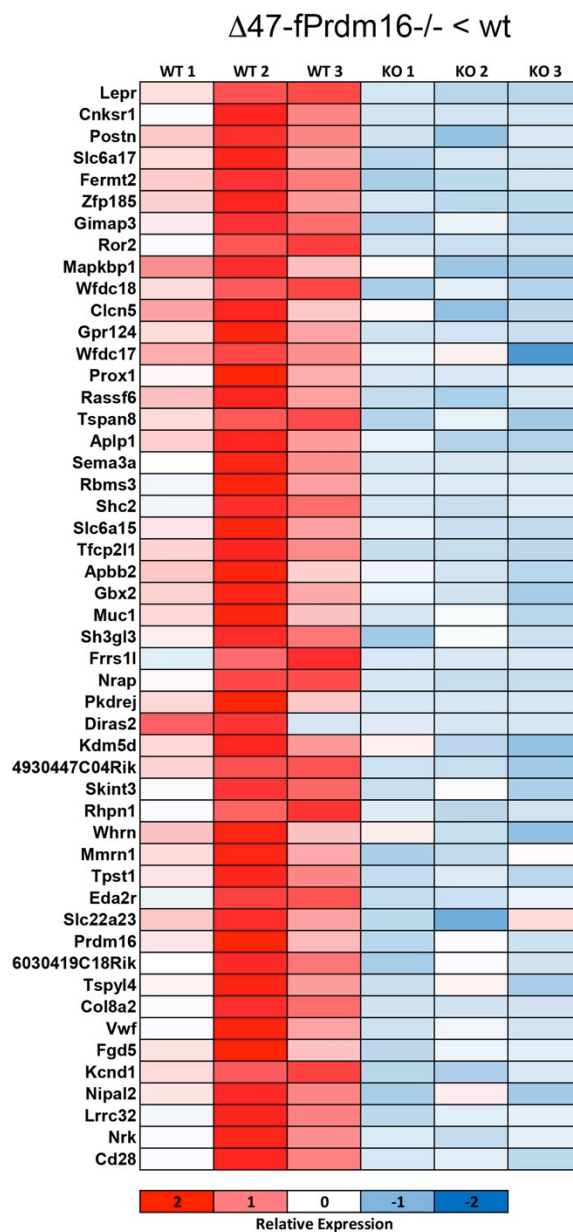
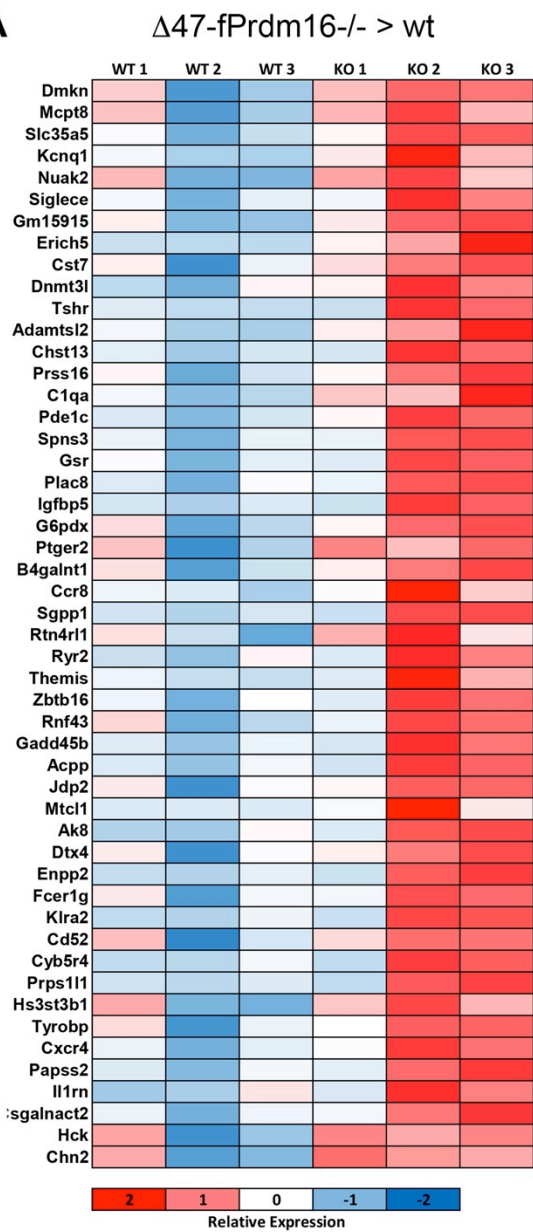
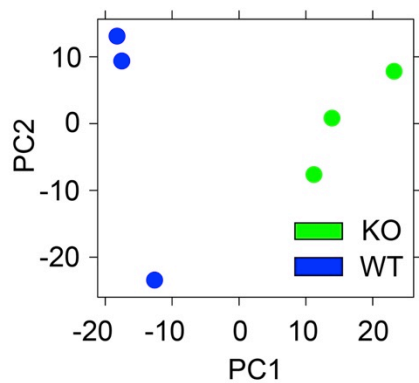


**Figure S5: Generation of *fPrdm16*<sup>-/-</sup> mice. (A)** Map of the 47bp and 13bp deletions (in red) obtained from mice using CRISPR/Cas9 pronuclear injection. **(B)** Comparison of the frameshifted amino acid sequence (red) leading to premature stop codons in both mice. **(C)** Subtractive qPCR quantification of *Prdm16* isoform mRNA copy number from  $\Delta 47$ -*fPrdm16*<sup>-/-</sup> mice (KO) and WT littermates shows selective loss of *fPrdm16* in the mutants. **(D)** Calculation of *fPrdm16* and *sPrdm16* RPKM obtained by subtracting Exon 1-3 RPKM (specific *fPrdm16* RPKM) from Exon 1-17 RPKM (total *Prdm16*) to calculate *sPrdm16* RPKM. **(E)** Mendelian distribution of E13-15 embryos of  $\Delta 47$ -*fPrdm16* mice ( $n = 62$ ). **(F)** Percent donor CD45.2 cells in BM of recipient mice 24 hours after transplantation of FL cells from either  $\Delta 47$ -*fPrdm16* (*fPrdm16*<sup>-/-</sup>) or WT littermates. ( $n = 5$  recipient mice). (n.s. =  $P > 0.05$ )

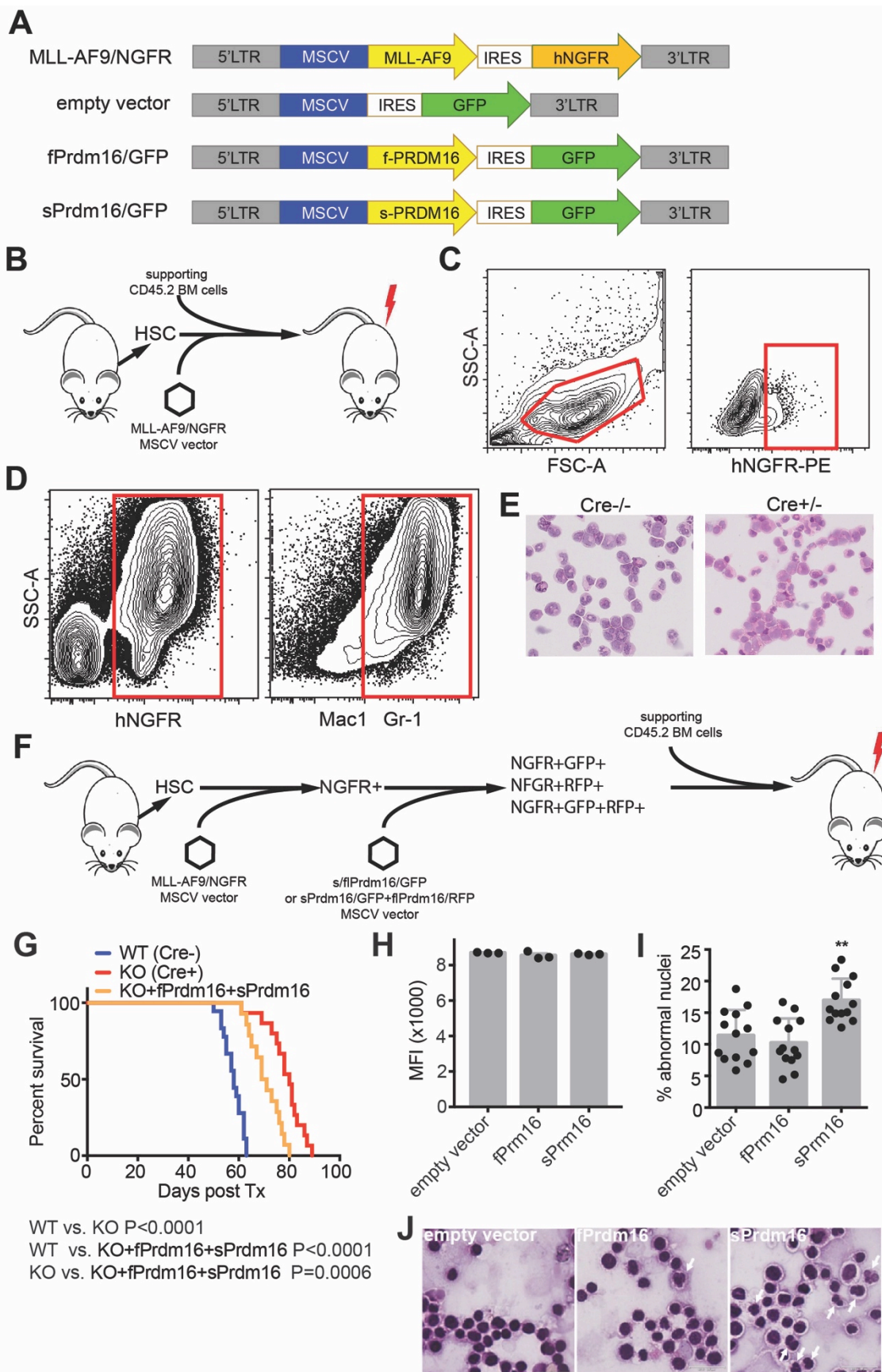




**Figure S6: Function of *fPrdm16*<sup>-/-</sup> HSCs.** (A) LSK frequency in FL of *fPrdm16*<sup>+/+</sup> (WT), *fPrdm16*<sup>+/-</sup> (HET), and *fPrdm16*<sup>-/-</sup> (KO) mice from  $\Delta 47$ -*fPrdm16*<sup>-/-</sup> or  $\Delta 13$ -*fPrdm16*<sup>-/-</sup> mice. (B) Percent Ki67<sup>+</sup> and (C) cleaved Caspase3<sup>+</sup> FL HSCs in  $\Delta 47$ -*fPrdm16*<sup>-/-</sup> and WT littermate embryos ( $n = 3$ ). (D) Donor repopulation in progenitor populations 16 weeks after competitive transplantation of  $\Delta 47$ -*fPrdm16*<sup>-/-</sup> or WT littermate FL cells, expressed as percent of CD45.2 donor cells within a progenitor population: LSK (Lin<sup>-</sup>Sca1<sup>+</sup>cKit<sup>+</sup>), CMP (Lin<sup>-</sup>Sca1<sup>-</sup>cKit<sup>+</sup>CD34<sup>+</sup>CD16/32<sup>lo</sup>), GMP (Lin<sup>-</sup>Sca1<sup>-</sup>cKit<sup>+</sup>CD34<sup>+</sup>CD16/32<sup>mid</sup>), MEP (Lin<sup>-</sup>Sca1<sup>-</sup>cKit<sup>+</sup>CD34<sup>-</sup>CD16/32<sup>lo</sup>), and CLP (Lin<sup>-</sup>Sca1<sup>lo</sup>cKit<sup>lo</sup>IL7ra<sup>+</sup>Flt3<sup>+</sup>) ( $n = 6$  recipients from 2 independent transplants). (E) Flow cytometry plots of donor-derived splenic B-cells 16 weeks after competitive transplantation of  $\Delta 47$ -*fPrdm16*<sup>-/-</sup> or WT littermate FL cells. (MZ: marginal zone B-cells; FO: follicular B-cells). (F) Histograms of SCA1 MFI in donor MZ B-cells illustrating higher Sca1 in the MZ B-cells from  $\Delta 47$ -*fPrdm16*<sup>-/-</sup> than from WT littermate FL cells.

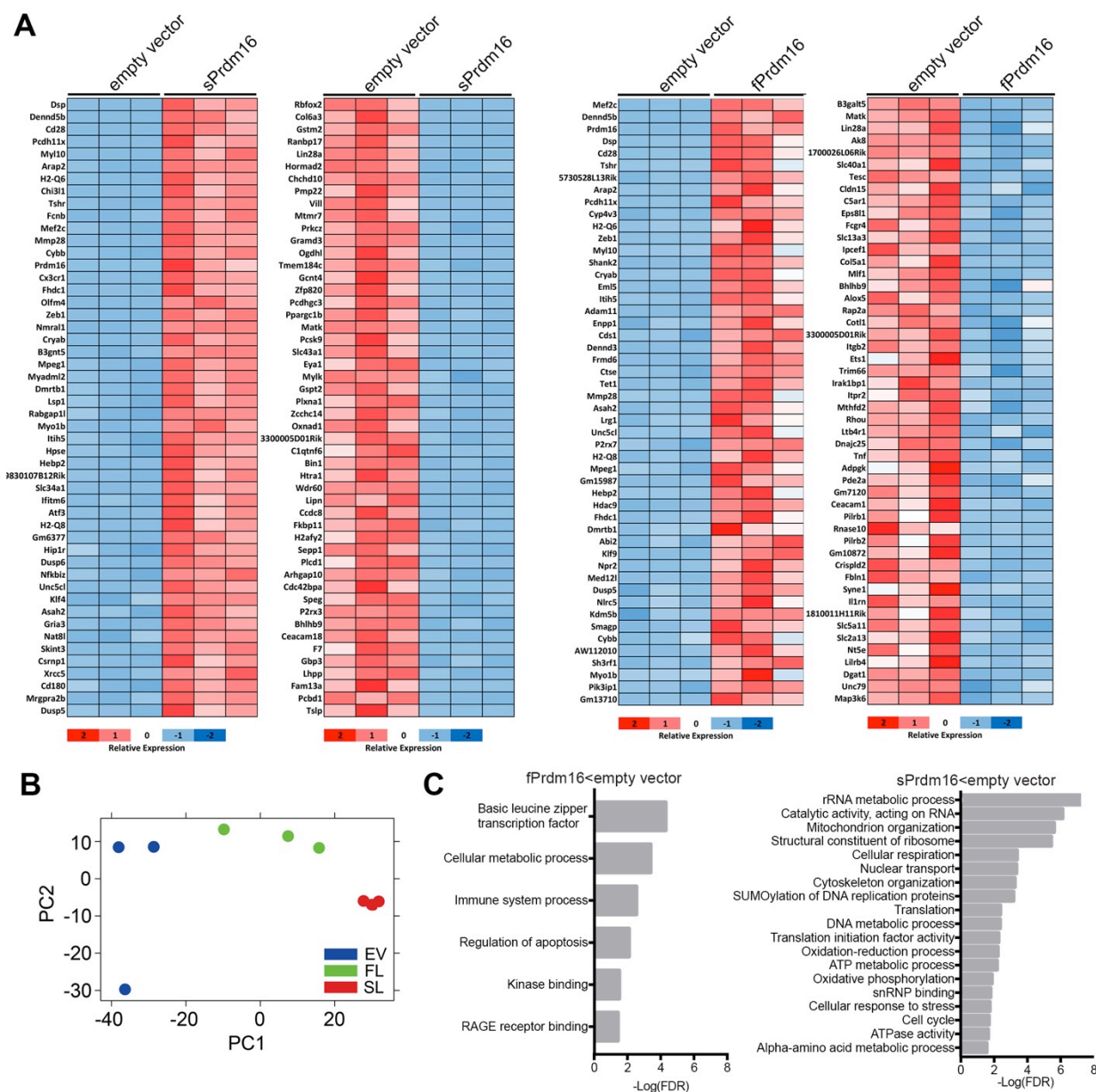
**A****B**

**Figure S7: Genome-wide expression analysis in *fPrdm16*<sup>-/-</sup> HSCs.** (A) Heatmap of the top 50 genes (by *P*-value) up/downregulated in  $\Delta 47$ -*fPrdm16*<sup>-/-</sup> (KO) FL HSCs compared to WT littermates, as determined by RNAseq. (B) Principal component analysis (PCA) of  $\Delta 47$ -*fPrdm16*<sup>-/-</sup> (KO) and WT littermate FL HSC RNAseq samples.



**Figure S8: Retroviral expression of *sPrdm16* and *fPrdm16* in MLL-AF9 leukemia.** (A) Maps of retroviral vectors used in MLL-AF9 leukemia studies. (B) Experimental design of MLL-AF9 leukemia studies. (C) Representative flow cytometry plot showing hNGFR expression after transformation of HSCs with hNGFR-MLL-AF9 retroviral vector. (D) Representative flow cytometry plot showing hNGFR and myeloid marker expression in PB of moribund mice at the endpoint of survival experiments. (E) Representative hematoxylin and eosin (H&E) staining of purified hNGFR<sup>+</sup> cells from moribund *Prdm16<sup>fl/fl</sup>.Vav-Cre* (Cre+/-) and WT littermate (Cre-/-) mice. (F) Schematic of MLL-AF9 transformation of HSCs and forced expression of *fPrdm16*-GFP, *sPrdm16*-GFP, or *sPrdm16*-GFP/*fPrdm16*-RFP. (G) Survival curves of lethally irradiated mice transplanted with either *Prdm16<sup>fl/fl</sup>.Vav-Cre*, WT littermate, or *Prdm16<sup>fl/fl</sup>.Vav-Cre* transduced with *sPrdm16*-GFP/*fPrdm16*-RFP hNGFR+ MLL-AF9 cells. ( $n = 15$  recipient mice in three independent experiments) (H) Quantification of GFP mean fluorescence intensity (MFI) of *Prdm16<sup>fl/fl</sup>.Vav-Cre* MLL-AF9 cells expressing either empty vector, *fPrdm16*-GFP or *sPrdm16*-GFP ( $n = 3$  MLL-AF9 lines). (I) Percent of cells with abnormal (elongated or multi-lobed) nuclei (by hematoxylin/eosin stain) in BM of leukemic mice transplanted with *Prdm16<sup>fl/fl</sup>.Vav-Cre* MLL-AF9 cells expressing either empty vector, *fPrdm16*-GFP or *sPrdm16*-GFP ( $n = 4$  fields from 3 independent mice, each field containing at least 50 BM cells, \*\* =  $P < 0.01$ , One-way ANOVA for multiple comparisons;). (J) Representative images of the data presented in (I). Arrows indicate abnormal nuclei.





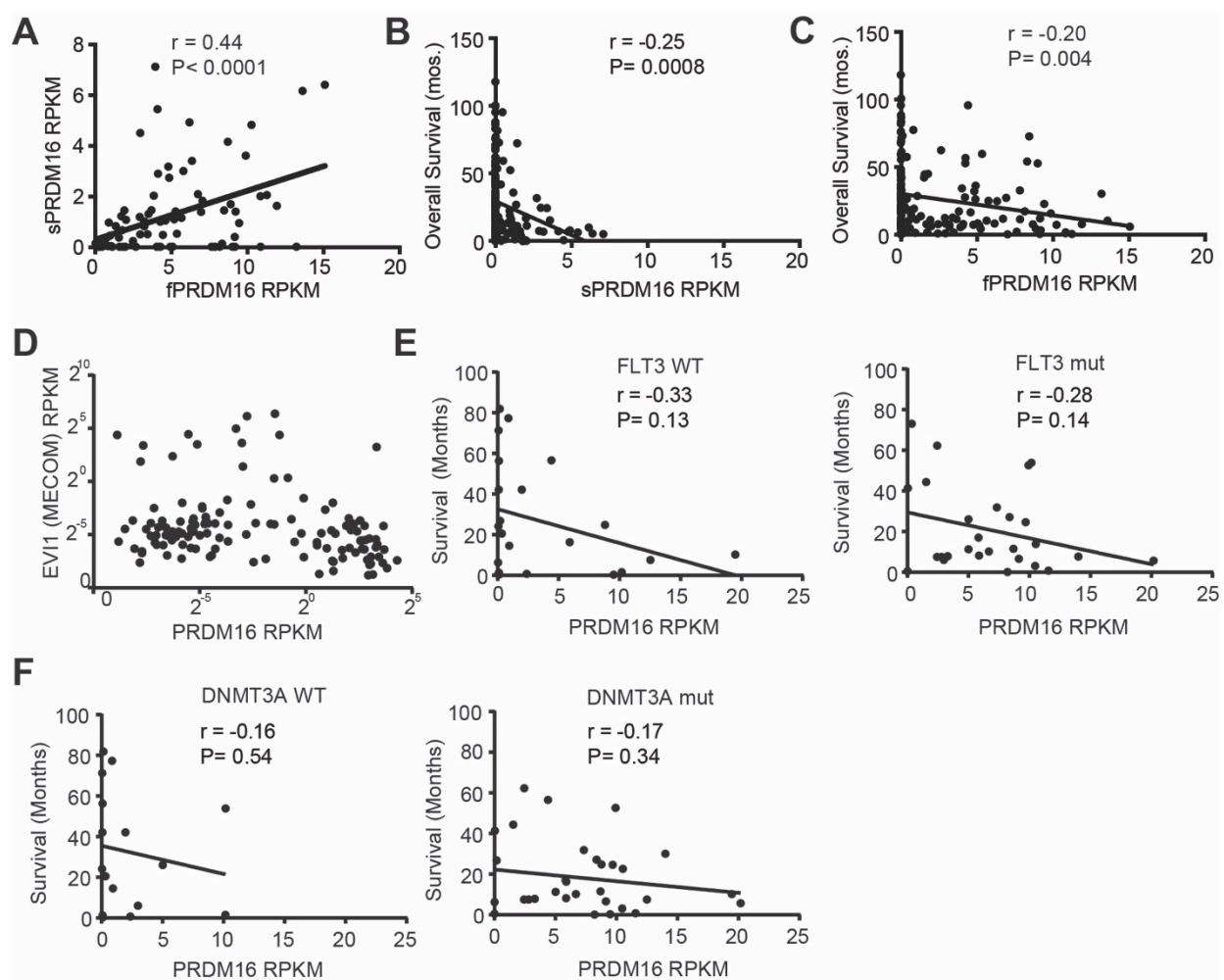


**Figure S10: Expression of *sPRDM16* and *fPRDM16* in CGA.** (A) Correlation between *fPRDM16* and *sPRDM16* mRNA expression (RPKM) among the set of *PRDM16*-expressing human AML cases in the Cancer Genome Atlas (CGA) cohort (corresponding to Q3 and Q4, or RPKM >0.1, as described in the manuscript and in Figure 7B) ( $n = 90$ ). (B,C) Negative correlation between both *sPRDM16* (B) and *fPRDM16* (C) mRNA expression (RPKM) and overall survival among 179 AML in the CGA. (D) Absence of correlation between *PRDM16* and *EV11 (MECOM)* RPKM among the 179 CGA cases ( $P = 0.44$ ). (E,F) Correlation between survival and *PRDM16* expression among *NPM1*-mutant AML with wt or mutant *FLT3* (E) or *DNMT3a* (F).